Vision 20/20: The role of Raman spectroscopy in early stage cancer detection and feasibility for application in radiation therapy response assessment

Suneetha Devpura,[a] Kenneth N. Barton, and Stephen L. Brown
Department of Radiation Oncology, Henry Ford Hospital, Detroit, Michigan 48202

Olena Palyvoda
College of Engineering, Wayne State University, Detroit, Michigan 48202

Steven Kalkanis
Department of Neurosurgery, Henry Ford Hospital, Detroit, Michigan 48202

Vaman M. Naik
Department of Natural Sciences, University of Michigan-Dearborn, Dearborn, Michigan 48128

Farzan Siddiqui
Department of Radiation Oncology, Henry Ford Hospital, Detroit, Michigan 48202

Ratna Naik
Department of Physics and Astronomy, Wayne State University, Detroit, Michigan 48201

Indrin J. Chetty
Department of Radiation Oncology, Henry Ford Hospital, Detroit, Michigan 48202

(Received 21 November 2013; revised 28 February 2014; accepted for publication 28 March 2014; published 18 April 2014)

Raman spectroscopy is an optical technique capable of identifying chemical constituents of a sample by their unique set of molecular vibrations. Research on the applicability of Raman spectroscopy in the differentiation of cancerous versus normal tissues has been ongoing for many years, and has yielded successful results in the context of prostate, breast, brain, skin, and head and neck cancers as well as pediatric tumors. Recently, much effort has been invested on developing noninvasive "Raman" probes to provide real-time diagnosis of potentially cancerous tumors. In this regard, it is feasible that the Raman technique might one day be used to provide rapid, minimally invasive real-time diagnosis of tumors in patients. Raman spectroscopy is relatively new to the field of radiation therapy. Recent work involving cell lines has shown that the Raman technique is able to identify proteins and other markers affected by radiation therapy. Although this work is preliminary, one could ask whether or not the Raman technique might be used to identify molecular markers that predict radiation response. This paper provides a brief review of Raman spectroscopic investigations in cancer detection, benefits and limitations of this method, advances in instrument development, and also preliminary studies related to the application of this technology in radiation therapy response assessment. [http://dx.doi.org/10.1118/1.4870981]

Key words: Raman spectroscopy, cancer, radiation therapy, tumor response, Raman peaks

1. INTRODUCTION

The phenomenon of Raman scattering was discovered by Sir Chandrasekhara Venkata Raman in 1928.[1] In this technique, a laser light of a certain frequency (ν_0) incident on a sample interacts with the molecules in the sample leading to scattering. Much of the incident light is scattered elastically (Raleigh scattering) while only a very small fraction of incident photons ($\sim$1 in 10×10^6) undergo inelastic scattering (Raman effect). The basic necessary condition for observing the Raman scattering is that the polarizability must change during vibrations of the molecules.[2] Figure 1 presents the energy diagram of Raman scattering processes. In Stokes Raman scattering [$h(\nu_0 - \nu_m)$, h is the Planck constant], the incident photon perturbs the molecule from its vibrational ground state to a virtual excited state which quickly decays into a higher vibrational state instead of the initial state thus leading to a loss energy of the incident photon.[2] Here, the energy is absorbed by the molecule ($h\nu_m$). If the scattering results in an excitation from an initial excited vibrational state to a virtual state and subsequent de-excitation to a ground state or a lower excited state than the initial state, then the emitted photon has more energy than the absorbed photon [$h(\nu_0 + \nu_m)$]—this is referred to as anti-Stokes scattering (see Fig. 1). Although, the emitted photon has higher energy, anti-Stokes Raman scattering produces low intensity Raman peaks relative to Stokes Raman scattering. Thus, the Stokes part of the spectrum is typically used. When the temperature increases, the probability of molecules existing in the higher vibrational states increases (depends on the Boltzmann distribution), and as a result the intensity of the anti-Stokes bands also increases. The energy difference between the incident photon

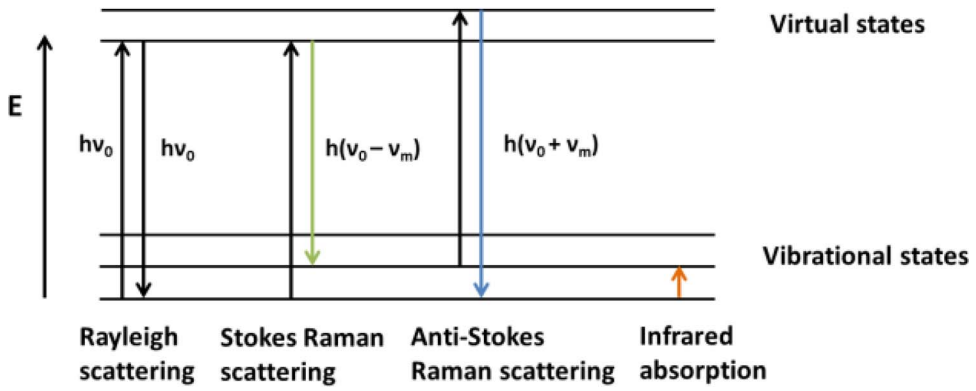

FIG. 1. An energy diagram of Rayleigh and Raman scattering processes.

and the Raman scattered photon is defined as the Raman shift (often expressed in wavenumbers, cm^{-1}). The Raman intensity depends on the polarizability of the molecule, the intensity of the laser source, and the concentration of active groups.[2] Infrared absorption occurs when the energy of the incident photon matches the natural frequency of a vibrational mode. A change in dipole moment of the molecule must occur for a vibrational mode of a molecule to be infrared active.[3] Raman scattering and infrared scattering cannot occur simultaneously in centro-symmetric molecules (molecules with a center of inversion symmetry, e.g., CO_2).[2] Therefore, these vibrational spectroscopic techniques can be used as complementary techniques for characterization of materials.

The principle behind confocal Raman microspectroscopy is same as the Stokes Raman scattering except the differences in the experimental setup.[4] This technique has the capability to acquire depth profiles in addition to spatial information about a region of interest. Surface enhanced Raman scattering (SERS) is another spectroscopic technique in which the intensity of the vibrational modes of the molecules adsorbed on rough metal surfaces is enhanced. Alternately, the use of metallic nanoparticles can enhance the Raman signal. These nanoparticles typically have reporter dyes adsorbed to the surface that produces characteristic SERS spectral outcome.[5] Gold and silver are the common types of nanoparticles used in such applications.[6] With the choice of a reporter dye (Raman active layer), the Raman band associated with a certain molecular vibrational mode is enhanced. If the incident laser frequency coincides with the energy of an electronic state, resonance Raman scattering can result. Coherent anti-Stokes Raman scattering is another method that uses multiple laser photons instead of a single laser excitation source to produce coherent intense Raman signals at anti-Stokes frequencies. This technique is mostly used in the laboratory use for single cell characterization through vibrations of chemical bonds and capable of high resolution cell imaging.[7]

Raman spectroscopy is an analytical optical spectroscopic method where, from the spectral output, one can infer information about the molecular composition of the target tissue. This technique detects the presence of specific biomolecules through their intrinsic vibrational modes and the intensity of the Raman peaks depends on the concentrations of those biomolecules under investigation. Cells are made of proteins, lipids, carbohydrates, and nucleic acids.[8] These molecular components, when functioning properly, work together in the chemistry of life. To work together, the molecular components must be present and active at specific times. Disease states are caused when the function and/or expression of molecular components becomes abnormal. Unfortunately, one abnormal molecular component can lead to other components also becoming abnormal. For example, when the proteins that maintain the stability of the genome fail to function properly, DNA aberrations build up resulting in more abnormal protein expression leading to more DNA aberrations in a vicious cycle. Cancer is a disease of DNA aberrations which translate into abnormal protein expression and eventually changes in other molecular components as well. As a result, the chemistry of the cell can be impacted significantly.[9] These chemical changes can take the form of new or unique signals associated with a disease state. Raman spectroscopy is well-suited to detect these changes in the molecular components that arise from disease.

1.A. Instrumentation and analysis techniques

Figure 2 shows a schematic of an experimental setup of Raman spectroscopy. If the incident light loses energy (Stokes Raman scattering), which decreases its frequency, that energy excites the molecular vibrations. The scattered light $(\nu_0 - \nu_m)$ then carries the information about the molecular structure. The scattered light from the sample (that passes through a filter to remove the Rayleigh peak) is collected and analyzed using a spectrometer which disperses the scattered light frequencies and produces a spectrum of scattered light as shown in Fig. 2. A set of scattered light frequencies contains information about the vibrational energy states of the molecule and thus provides a unique chemical fingerprint of the molecule.

In confocal Raman microspectroscopy, the microscope that is integrated into a spectrometer consists of a two pinhole aperture microscope configuration. The residual scattered light generated from out of focus points in the sample is removed by this configuration.[4] Moreover, the high quality optical microscopes provide high resolution imaging capabilities in this technique. If the microscope is replaced with a design of fiber-optic bundle that contains an excitation fiber

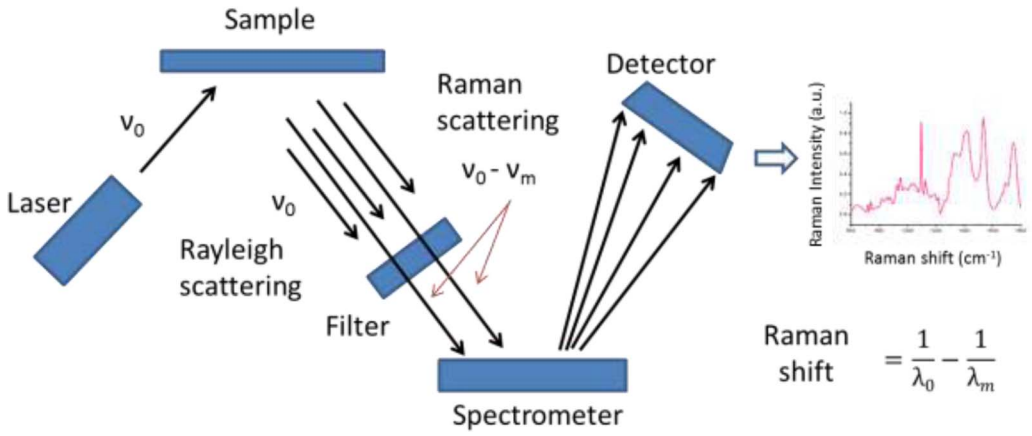

FIG. 2. A schematic diagram of an experimental set of Raman spectroscopy.

to deliver the incident light and the collection fibers to collect the scattered light, or so called a Raman probe, Raman spectroscopy becomes promising in application of easily accessible organ lesions *in vivo*.[10,11] The development of sensitive charge-coupled device detectors (CCDs) and diode lasers has increased the ability to explore Raman spectroscopy in material characterization using NIR excitation.[12]

When considering biological applications, the choice of wavelength is a key parameter. The sensitivity or the intensity of the Raman scattering, spatial resolution, and the effects of fluorescence background depend on the excitation wavelength. The intensity of the Raman signal depends on the inverse fourth power of the scattered wavelength, thus, lower the incident wavelength higher the intensity of the Raman signal. Additionally, the spatial resolution increases with the decreasing wavelength. However, the effect in fluorescence background is high in a lower wavelength laser excitation; therefore, near infrared laser sources are preferred.[2] In fact, the samples may tend to get damaged due to high energy laser photons (or use of low wavelength excitation). Often, the laser wavelength varies in the range of visible to near infrared such as 514.5 (argon-ion), 540.9, 647.1 (krypton-ion), 785 nm (diode lasers), 1064 nm (Nd:YAG), etc.[13] The wavelength in the ultraviolet range (e.g., 244 or 364 nm) is also possible to target specific molecules by using their intrinsic excitation wavelength (resonance).[14] The availability of hand-held spectrometers aids portable Raman spectroscopy, but these techniques with such spectrometers often have low signal to noise ratio compared to the Raman systems equipped with liquid nitrogen cooled or thermoelectrically cooled CCDs.[14]

The calibration procedures involve calibration of the Raman instrument, spectral processing (smooth and background signal removal), and spectral normalization. Prior to the data acquisition, the status of the instrument is routinely checked; calibration of the spectrometer is usually performed using a known sample, e.g., silicon, naphthalene, barium sulfate, tungsten, etc. Once the spectra are acquired the processing of the data is essential. As the Raman signal contains a fluorescence background that can obscure the biomarker signal, a function, for example, a fifth order polynomial[15,16] is typically fit to the data and the background signal subtracted and smoothen so that the spectrum can be more clearly distinguished. Then, the normalization of the spectrum is done based on the researcher's preference; one may normalize the spectrum to the maximum intensity peak or a selected Raman peak[15,16] or the area under the curve.[17] Once the data are processed, then the interpretation of the biochemical changes (chemical analysis) present in different groups of spectra is performed. The Raman spectral range of 600–1800 cm^{-1} is considered as the "biological window" because it contains most of the fundamental active modes of biological molecules. Biochemical information is extracted from the Raman spectra and the spectral differences are analyzed by quantitative multivariate analytical techniques. Both these approaches assist the interpretation of the Raman spectra of any specific state of histopathology.

The band frequencies and their intensities in a Raman spectrum contain the chemical information about the molecular composition of the sample and the concentrations of molecules that make-up the sample. These Raman peaks are assignable to unique vibrational modes which can be found in the literature.[19,20] Figure 3 represents the molecular

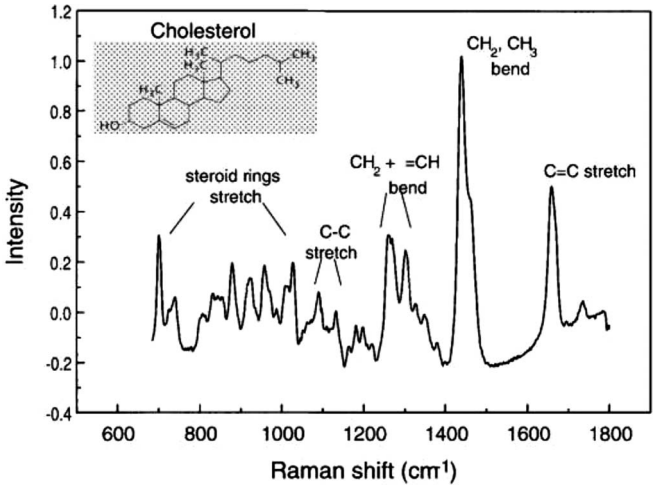

FIG. 3. Near IR Raman spectrum of cholesterol indicating vibrational bands. Reproduced by permission from E.B. Hanlon, R. Manoharan, T. W. Koo, K. E. Shafer, J. T. Motz, M. Fitzmaurice, J. R. Kramer, I. Itzkan, R. R. Dasari, M. S. Feld, "Prospects for in vivo Raman spectroscopy," Phys. Med. Biol. **45**(2), R1–59 (2000) © Institute of Physics and Engineering in Medicine. Published on behalf of IPEM by IOP Publishing Ltd. All rights reserved.

fingerprint of cholesterol along with general assignment of the bands to localized group vibrations of the molecule. The information of Raman peak height and the position enables identifying a particular state of a tissue. This chemical information provides an insight into an unknown pathology and these Raman signatures infer the existence of increment or decrement of certain active chemical species through visual observation of average Raman spectra. Moreover, a quantitative analysis can be carried out by determining the relative Raman intensity differences between different categories.[21] In fact, certain biomarkers can be selected by using reference Raman spectra in their pure form as shown in Fig. 3.

Classification problems involving biological tissue require gold-standard verification typically using histology, e.g., representative spectra from known cases are compared with that from normal tissue to determine biomarkers of potential interest. A Raman spectrum may consist of multiple biomarkers. Thus, one may generate the measured Raman signal using the biomarkers (or Raman signatures) in their pure form. Visual observations for the presence of certain biomarkers are possible. There are custom software programs designed for the purpose of identifying biomarkers of known pathology. Haka *et al.*[22] utilized reference Raman spectra in pure substance to compose multiple biomarkers and regenerate the measured signal. In this study, breast tissues with normal, fibrocystic change, fibroadenoma, and infiltrating carcinoma were investigated using data from 58 patients. The average power illuminated at a tissue volume of $\sim$1 mm^3 varied between 100 and 150 mW with an 830 nm laser. Nine reference Raman spectra were used to construct the measured tissue signal and arriving at the chemical composition.

Figure 4 demonstrates mean Raman spectra of each pathological state (both measured and reconstructed), and their corresponding H&E stained tissue images. The model fit coefficients of nine reference spectra are included in Fig. 4 and these values depend on the concentration of a particular model component and the strength of the signal at unit concentration. The residual spectra reflect that the model accounts for majority of the spectral content. The key diagnostic parameters were fat and collagen basis spectra. This investigation is the first report of spectral-based algorithm to identify breast tissues and their specific pathological states.

Commonly used multivariate analytical techniques in Raman spectral identification are principal component analysis (PCA)[23] and discriminant function analysis (DFA).[24] As the Raman spectra contain multiple variables with differing intensities (e.g., 601 variables in 600–1800 cm^{-1} range with a 2 cm^{-1} interval), PCA reduces the number of variables and captures the maximum information in the spectral output. These new variable or principal components (PCs) could be used as predictors or used in subsequent DFA analysis.[23] When these PCs are plotted one may observe trends in the data. DFA classifies the Raman data into independent groups by maximizing the variation between the groups while the variation within each group is minimized. This technique calculates discriminant functions (a linear function with discriminating variable where the coefficients are determined by satisfying certain conditions),[24] one less than the groups of the data. The first discriminant function contains the maximum variance in the data; the second discriminant function contains the next maximum variance in the data, and so forth. Based on the analysis, each spectrum has discriminant scores associated with each discriminant function. If these discriminant functions are plotted, then the distinct pathological groups can be observed. Moreover, these discriminant scores are used to classify the data into independent categories. Leave one out classification method is preferred for biological application as it tests each Raman spectrum against the rest of the data set and assigns the spectrum to a particular group based on its DF score. The other statistical techniques used for Raman data classification are support vector machines,[25] neural networks,[26] etc. Often, Raman spectral features are distinct among different groups; however, if subtle spectral differences are observed, the need for multivariate statistical analyses is crucial. These statistical techniques provide rapid quantitative identification of a pathological state *in vivo*.

Raman spectroscopy has been shown to be helpful in diagnosing cancerous from normal cells and, in the future, Raman spectroscopic approaches might advance to the point of being able to provide rapid minimally invasive real-time diagnosis. Among commonly used optical molecular diagnostics such as fluorescence, reflectance, and elastic scattering—Raman spectroscopy provides the most detailed chemical information about a tissue sample.[18] With the advancement in optical technology, it is becoming desirable to have noninvasive and reliable optical detection methods whose results are interpreted objectively. Raman spectroscopy is well suited for these purposes and can be used as a molecular diagnostic tool, clinically. More details of development and advances of Raman spectroscopy can be found in other publications.[6,27–30]

1.B. Raman spectroscopy for early stage cancer detection

Understanding the physical properties of tumors might provide a window into more fundamental understanding of how the tumor progresses and responds to therapies. Indeed, one of the 20 provocative questions posed by Dr. Harold Varmus of the National Cancer Institute in 2012 was: "*How can the physical properties of tumors, such as a cell's electrical, optical, or mechanical properties, be used to provide earlier or more reliable cancer detection, diagnosis, prognosis, or monitoring of drug response or tumor recurrence?*."[31] Raman spectroscopy can be used to characterize the biochemical properties of cells. In the context of tumors, because the cell structure changes as tumor becomes differentiated, the Raman technique can be used to be able to characterize different stages in the progression of a cell, from normal to cancerous. Raman spectroscopy has been extensively investigated for classification of onset of tumors and their progression by many researchers in different organs including prostate,[32–35] breast,[22,36–39] bladder,[40,41] brain,[42–46] and skin.[47–50] Crowe *et al.*[32,33] investigated benign and malignant prostate biopsies and were able to observe an overall accuracy of 89% for each

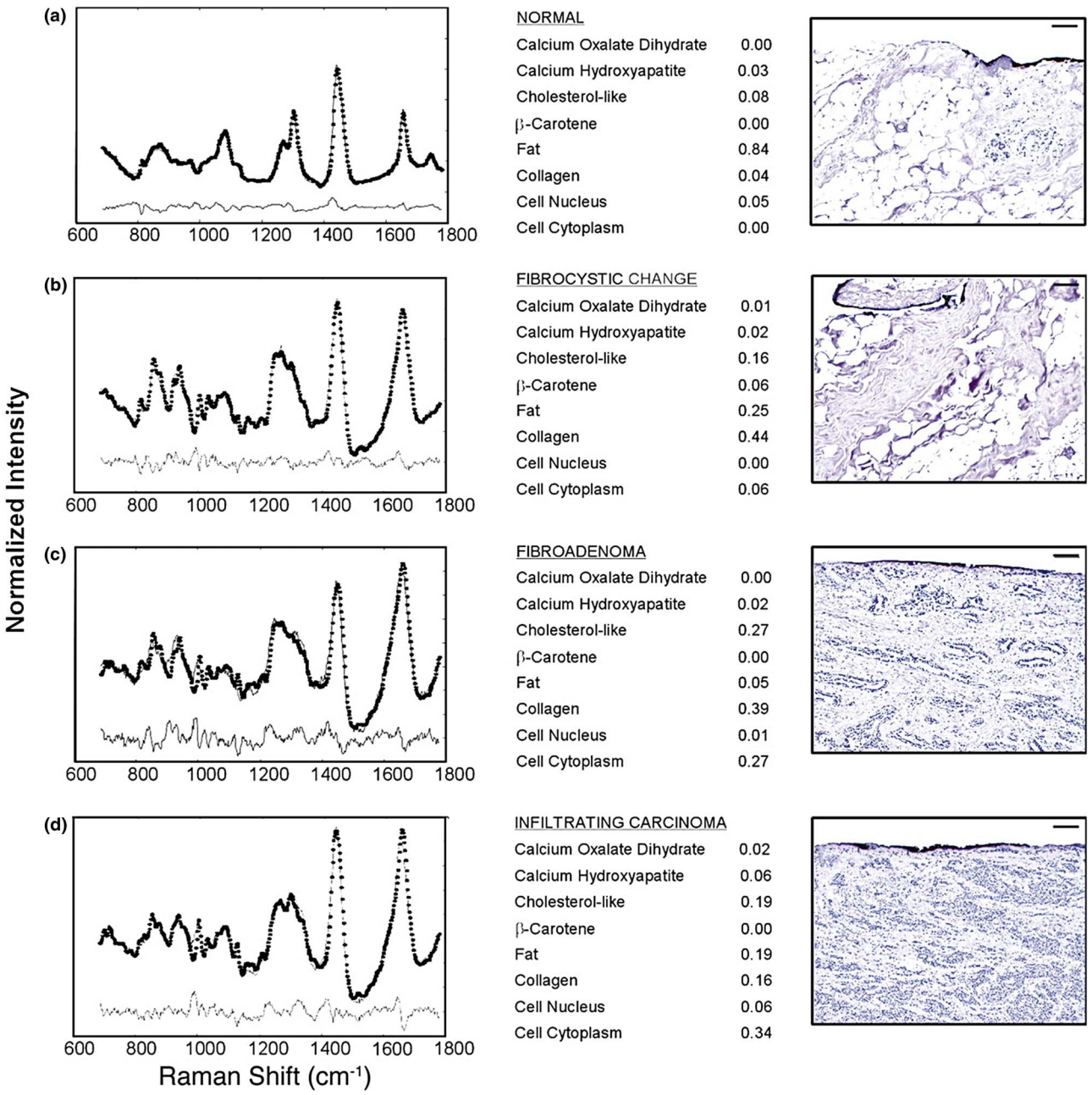

FIG. 4. Normalized Raman spectra (solid lines), model fits (dotted lines), residuals (shown below the spectrum), fit coefficients, and images from hematoxylin/eosin (H&E)-stained sections used to make the histopathology diagnosis for normal breast tissue (a), fibrocystic change (b), fibroadenoma (c), and infiltrating carcinoma (d). The India ink used to record the region of spectral examination is seen as a black line on the tissue surface in the H&E images (scale bars, 100 μm). Reproduced by permission from A. S. Haka, K. E. Shafer-Peltier, M. Fitzmaurice, J. Crowe, R. R. Dasari, and M. S. Feld, "Diagnosing breast cancer by using Raman spectroscopy," Proc. Natl. Acad. Sci. 102, 12371–12376 Copyright (2005) National Academy of Sciences, U.S.A.

group, relative to pathological diagnosis. Similar results were found in subsequent Raman investigations.[34,35]

Stone *et al.*[35,40] reported the potential of using Raman spectroscopy in several cancer types; prostate, bladder, breast, esophagus, and colon cancer. For this study, frozen specimens were investigated in their benign and malignant states using a customized Renishaw Raman spectrometer. The spectra were acquired by irradiating 2–3 μm area with a power of 31 mW using an 830 nm laser excitation. Figure 5 shows mean Raman spectra of each pathological group in their benign and malignant states. The spectra were corrected to the energy sensitivity of the spectrometer and were normalized to the mean intensity. The Raman spectra indicated substantial spectral differences in pathology, e.g., Raman peaks demonstrated higher levels of glycogen, tryptophan, tyrosine, proline, and proteins with α-helix structures in benign tissue of esophagus. The Raman spectra were analyzed using diagnostic predictive models constructed and optimized using principal component analysis and discriminant function analysis. The results of these multivariate spectral predictive models depicted more than 91% sensitivity and specificity for each epithelial cancer type. The results were suggestive that identifying early

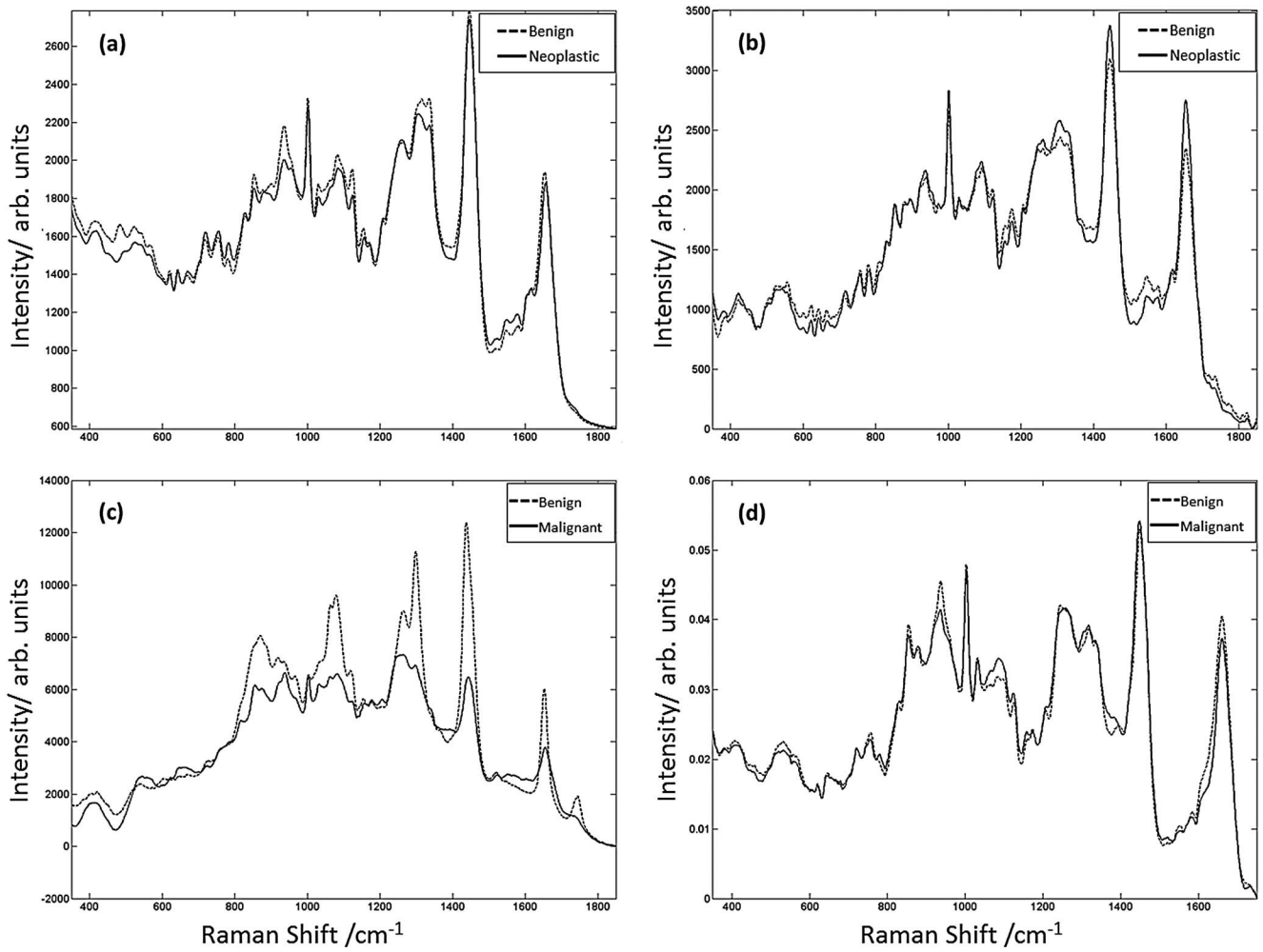

FIG. 5. Mean spectra from benign (dotted line) and neoplastic/malignant (solid line) tissue. (a) Esophagus; (b) colon; (c) breast; (d) prostate. Reproduced by permission from N. Stone, C. Kendall, J. Smith, P. Crow, and H. Barr, "Raman spectroscopy for identification of epithelial cancers," Faraday Discuss. 126, 141–157 (2004). Copyright (2004) Royal Society of Chemistry.

stage malignancies *in vivo* using Raman spectroscopy was feasible.

Haka *et al.*[22] performed *ex vivo* frozen breast cancer tissue Raman spectroscopic investigation and *in vivo* Raman measurements during partial mastectomy breast surgery were also investigated with a fiber optic Raman probe.[36] Both the *ex vivo* and *in vivo* Raman spectral data were in a good agreement[22,36] and the feasibility of Raman spectroscopy for intraoperative margin assessment, thereby inferring that the re-excision surgeries from positive margins determined by Raman signal can be reduced in partial mastectomy breast.[36] In a subsequent study, freshly excised normal, benign, and malignant breast cancer tissues were also examined, and a diagnostic algorithm was developed to stage the cancer.[37] Madjumder *et al.*[39] conducted a breast cancer tissue investigation using several optical techniques including Raman spectroscopy, fluorescence, and diffuse reflectance spectroscopy. They found that Raman spectroscopy offers superior diagnostic capability compared to fluorescence and diffuse reflectance spectroscopy.[39]

Bladder samples with different pathologies including normal bladder, cystitis, carcinoma *in situ* (CIS), transitional cell carcinoma, and adenocarcinoma were tested using Raman spectroscopy.[40,41] These different stages of bladder tissues were identified with high sensitivities and specificities. Koljenovic *et al.*[42] performed Raman measurements in glioblastoma and the necrotic tissues as the tumor grade can be inferred from the necrotic cells. They observed high levels of cholesterol in necrotic tissue. Krafft *et al.*[43] reported higher levels of lipid in normal brain tissues relative to intracranial tumors. Intracranial tumors showed higher levels of hemoglobin and the ratio of lipid to protein was low in these tumors. Based on the Raman spectral features, high content of lipid and protein was evident in normal dura relative to meningioma in dura matter.[43,44] Similar results were reported by Kalkanis *et al.*[46] that normal gray matter contains high levels of lipid and glioblastoma multiforme showed lower level of lipid content in comparison with normal brain tissues. In addition, necrotic tissues revealed strong contributions from proteins. A recent study performed an investigation of brain tumors with two optical techniques, attenuated total reflection Fourier-transform infrared (ATR-FTIR) and Raman spectroscopy.[45] The results suggested that either one of the techniques can be used to discriminate

normal brain or tumors when coupled using discriminant analyses. However, Raman spectroscopy has the advantage of providing the ability to perform tissue measurements with minimal preparation whereas tissue samples should be in dry form to obtain ATR-FTIR spectroscopy measurements. The presence of water molecules in a target has a minimal effect as water produces weak Raman scattering unlike in infrared absorption spectroscopy. As expected, Raman spectra obtained from dermal tissues showed strong resemblance of collagen spectra.[47] However, collagen content in the spectral features was lower near the tumor areas of basal cell carcinoma.

Lui *et al.*[48] performed real-time Raman spectroscopic evaluations of skin lesions (benign and cancer) in 453 patients between 2003 and 2011 using a hand-held Raman probe. This hand-held Raman device, "Verisante Aura" (developed by British Columbia Cancer Agency and the University of British Columbia) is now available for skin cancer diagnosis in Canada, Europe, and Australia, and though the system has not yet received FDA approval in the USA.[49] This hand-held Raman probe consists of a 785 nm diode laser source and focused onto a circular area of diameter 3.5 mm. The larger skin lesions were measured up to 3 times within the lesion with one second integration time. The resolution of this Raman probe is 8 cm^{-1}. Promising findings of this new device conclude that Raman spectral range 500–1800 cm^{-1} is optimal to classify skin cancer and/or precancerous from benign cells, 1055–1800 cm^{-1} is optimal for distinguishing melanoma from nonmelanoma, and Raman spectroscopy is not influenced by the body site of the head and neck melanoma and nonmelanoma lesions.[48] Recently, the same company has launched a new spectrometer called "VRS—Verisante Research System" and claimed to be the fastest Raman spectrometer. In addition, for research purposes another Raman probe called "Verisante Core" is currently available for lung, colon, and cervical cancer investigations and this probe is not FDA approved yet.[51] These developments aid the *in vivo* Raman spectroscopic assessments and provide means to implement real time diagnosis of early stage cancers in the future. In another study, 95% overall accuracy was observed for basal cell carcinoma, squamous cell carcinoma, inflamed scar tissue, and normal tissue *in vivo*.[50]

There are other major Raman spectroscopic methods used in the field including, SERS, resonance Raman spectroscopy, confocal Raman microspectroscopy, and coherent anti-Stokes Raman scattering (CARS). *In vivo* tumor targeting and detection can be achieved using nontoxic gold nanoparticles using SERS.[52] Animal studies were performed using SERS with nano tags and with penetration depths up to 1–2 cm. Vo-Dinh *et al.*[53] reported a cancer gene detection using a SERS method. Nanostructured metallic substrates were used as SERS active substrates to detect DNA targets without radioactive labels. Solid catalysts and catalytic reactions were mostly investigated using resonance Raman spectroscopy.[54] Confocal Raman microspectroscopy has been used for detection of skin lesions due to improvement in spatial resolution and penetration depths. Caspers *et al.*[55] characterized skin structure by combining confocal scanning laser microscopy with confocal Raman microspectroscopy to precisely target subsurface of the skin structure including sweat duct, sebaceous gland, and dermal capillary. Choi *et al.*[56] reported dermatological diagnosis of basal cell carcinoma using this technique. Raman spectral differences were observed in the amide I band (1589 cm^{-1}) and the PO_2^- symmetric stretching band (1085 cm^{-1}) between the skin lesions and the surrounding normal tissues. Coherent anti-Stokes Raman scattering provides vibrational imaging capabilities with high sensitivity and spatial resolution. This technique has been mostly used to characterize lipid, skin, and spinal tissues.[57,58] With the improvement in fiber optic probes, ultraviolet resonance Raman scattering has been used in applications such as saliva, urine,[30] and colon cancer.[59,60]

In a recent rat brain tumor study, investigators reported that a stimulated Raman scattering method was able to detect the tumor margin based on the lipid and protein content present in the tumor and the surrounding tissue.[61] The investigators performed a web-survey with three neuropathologists using a series of 75 Raman images and the corresponding 75 H&E stained images.[61] The pathologists were able to identify normal, infiltrating glioma, and high-density glioma in Raman images with greater than 98% accuracy relative to H&E pathology diagnosis. There have been several other promising Raman spectroscopic results reported in the literature for diagnosis of early stage cancer such as oral, cervix, pancreas, lung, etc. using Raman spectroscopic techniques.[17,62–70]

In an exploratory work, we were able to differentiate cancer from normal tissues by measuring biomarkers specific for head and neck squamous cell cancers using a total of 401 Raman spectra from 17 tissues.[71] The results show that Raman spectroscopy can be successfully used to identify specific biochemicals predictive of the presence of normal, preinvasive, and invasive cancers in human tissues with a high degree of accuracy (91.4%, 90.9%, and 88.8%, respectively) relative to pathological diagnosis. We found that cancer progression was related to tryptophan and keratin levels present in the tissues. Changes in relevant Raman intensities were observed, as shown in Fig. 6. In a pediatric tumor study, we found that Raman fingerprints associated with lipid, β-carotene, lipid, and cholesterol showed prominent suppression in ganglioneuroma and neuroblastoma in comparison with normal adrenal tissues.[72]

1.C. Raman spectroscopy for radiation therapy response assessment

Raman spectroscopy is fairly new to the field of radiation therapy. Tumor response to radiation therapy and normal tissue toxicity can vary from patient to patient.[73,74] Understanding the mechanical properties of tumor and normal cells using Raman spectroscopy might therefore lead to a better understanding of how they respond to therapy. Normal tissue dose tolerances limit the choice of dose to tumor leading to a balance between tumor control and normal tissue toxicities. The ability to identify molecular markers that predict radiation response and use that information to modify radiation treatment

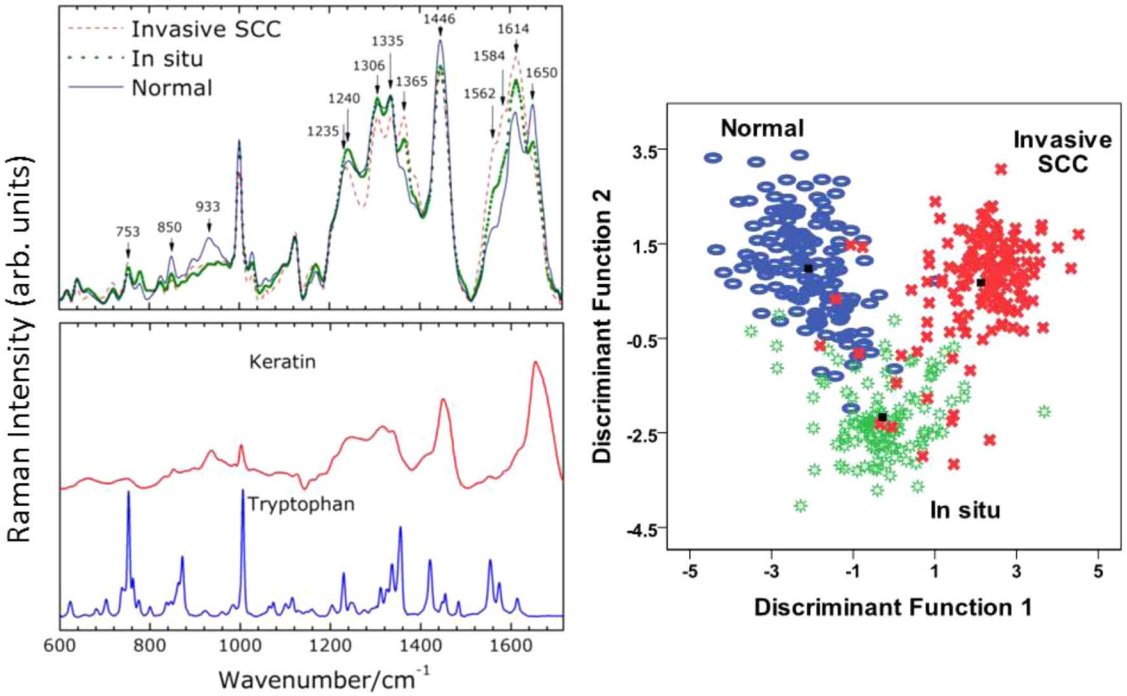

FIG. 6. (Left) Average Raman spectra of normal, carcinoma-*in situ*, and invasive squamous cell carcinoma with keratin and tryptophan Raman signal. (Right) Discriminant function analysis plot of the Raman data.[71]

has the potential to improve patient outcomes by tailoring the dose regime. Markers that are easily identifiable, immediately available, diagnostic and prognostic, and specific for a given disease or a patient are the most useful and promising to the radiation therapy field.[75] Raman spectroscopy, which probes microscopic properties of cells, is well suited toward possibly identifying such markers and their roles in radiation therapy.

With regard to the use of Raman spectroscopy for assessing therapeutic response, we will summarize the efforts of investigators who have published Raman spectroscopic results related to this topic. Mathews *et al.*[76] reported that multiple cell lines showed significant differences between treated and untreated cells using various dosing schemes. Human prostate cell lines were found to be radiosensitive whereas breast and lung cells seem to be radio resistant.[77] Radiation induced spectral changes were observed in Raman peaks associated with aromatic amino acids, conformation of protein structures, certain nucleic acid, and lipid functional groups. Lakshmi *et al.*[78] noted a small loss of lipid in trabecular regions with no osteoradionecrosis and a complete loss of lipid in osteoradionecrosis bone in oral cancer patients treated with radiation therapy. They also observed immediate structural changes in the inorganic normal bone matrix. Vidyasagar *et al.*[79] observed Raman spectral changes associated with radiotherapy response in cervix cancer patients before and 24 h after second fraction of radiation treatment. Although, minor Raman spectral changes were observed, it was noted that these results could be improved with high resolution Raman spectra.[79]

In the context of brain tissues, Lakshmi *et al.*[80] reported radiation induced Raman spectral changes in normal mice brain tissues. A single fraction, 10 Gy dose was delivered to the brain and Raman measurements were carried out at various time points after irradiation. The Raman measurements were also performed in muscle tissues after inducing stress by injections and restraint at different time points, and also 10 Gy postirradiation to the brain. The white-matter appeared to recover within a week after irradiation relative to gray matter. The Raman spectra of muscle tissue 30 min after stress were very similar to the muscle tissue when 10 Gy dose was delivered to the brain. This study infers that protective mechanisms are likely to function throughout the body, and as a result spectral changes were evident at sites remote from the site of the irradiation.[80] Morris *et al.*[81] performed a Raman spectroscopic investigation to determine the prolonged alterations in bone chemistry due to radiation. Animals subjected to unilateral localized hind limb irradiation with 20 Gy in four daily fractions showed significant increase in collagen crosslink ratio (1660/1683 cm^{-1}) at 1, 4, 8, 12, and 26 weeks in postirradiation. Degradation of collagen integrity was also reported in human cortical bone due to radiation.[82] The radiation induced abnormalities in bone mineral were evident in Raman spectral features one week after irradiation and persisted for 26 weeks which is in agreement with a previous study.[78] In another study, amifostine (AMF), a radioprotective compound was tested using Raman spectroscopy in rats.[83] A cohort of rats received AMF subcutaneously 45 min prior to radiation (five-day fractionated dose of 70 Gy). The left mandible was tested and compared relative to a group with 70 Gy irradiation in five fractions without AMF treatment and a control group with no irradiation. The Raman spectroscopic results suggested that AMF maintains and protects the bone mineral quality from radiation damage.[83]

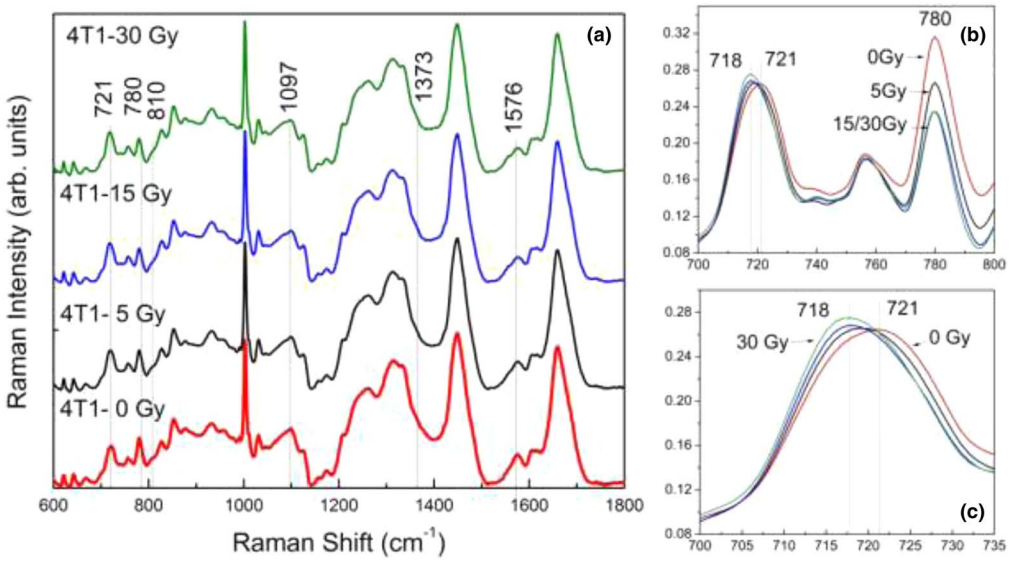

FIG. 7. (a) Mean Raman spectra of untreated (0 Gy), 5, 15, and 30 Gy; (b) DNA/RNA intensity suppression; and (c) Raman peak shift of 721–718 cm^{-1}.

2. PRELIMINARY RESULTS OF RADIATION THERAPY RESPONSE IN MURINE BREAST CANCER CELLS *IN VITRO*

To the best of our knowledge, the data presented in this section are the first report of *in vitro* assessment of tumor response to radiation therapy in 4T1 mouse breast cancer cells using Raman spectroscopy. Multiple dose regimens were used to determine the dose which best correlated the Raman signal with tumor response. 4T1 mouse breast cancer cells were plated in 60 mm dishes and after 48 h irradiated to doses of 5, 15, and 30 Gy using a cesium irradiator. The cells were lifted using trypsin-EDTA and resuspended in PBS (phosphate buffer saline) 48 h in postirradiation. The Raman measurements were carried out on untreated (0 Gy) and treated cancer cell samples (5, 15, and 30 Gy) per fraction, in single fractions. Measurements were repeated. A Raman microscope-spectrometer (Renishaw Inc., UK) with a 785 nm laser excitation source was used to record the Raman spectra. With a 50× objective, the laser light was focused onto an area of $2 \times 20\ \mu m^2$ to excite the molecules in the cell samples. Each Raman spectrum was acquired with 10 s exposure time with two accumulations. A total of 160 Raman spectra were collected (~40 cells from each group). The Raman data were processed to reduce the noise and the background fluorescence using a custom MatLab program that uses an adaptive minmax wavelet method.[16] Principle component analysis[23] (PCA) and discriminant function analysis[24] (DFA) were used to analyze and interpret the data. PCA captured 97% of the variance in the spectral range 600–1800 cm^{-1} (Raman intensities at each 2 cm^{-1} interval) and reduced the number of independent variables in the Raman spectroscopic data into 20 principal components (PCs). These new variables were used as input variables for the DFA. The DFA technique classifies the Raman data into independent groups, such as in producing distinct clusters, the intragroup variation is minimized, and the intergroup variation is maximized.

A mean Raman spectrum was generated for each group [Fig. 7(a)]. Several Raman peaks showed prominent spectral changes between groups. The Raman peaks associated with DNA/RNA (Refs. 19 and 84) [e.g., 780 cm^{-1} in Fig. 7(b)] showed a systematic suppression as the dose level was changed from 0 to 30 Gy. This indicates that the chemical changes occurring in DNA/RNA molecules due to radiation are prominent. It is interesting to note that the 721 cm^{-1} DNA Raman peak showed a significant ($p < 0.001$) shift of ~3 cm^{-1} at 0.05 confidence interval between untreated and 15 Gy/30 Gy 4T1 cells [Fig. 7(c)] indicating structural changes to the DNA.

These results suggested that radiation damage at the cellular level translates to observable changes in the Raman spectra. In addition to the peak shown in Fig. 7(b), the Raman peaks associated with DNA/RNA (Refs. 19 and 84) at 810, 1097, 1373, and 1576 cm^{-1} [see Fig. 7(a)] also showed suppressions in treated tumor cells (15 or 30 Gy) relative to the untreated breast cancer cells. The statistical analysis showed distinct clusters for all four groups as shown in Fig. 8(a) where each point represents a Raman spectrum. Figure 8(b) shows the analysis considering only, untreated (0 Gy) and treated (15 and 30 Gy) groups. These spectral changes are responsible for the high degree of accuracy in treated (96.3%) vs untreated (94.6%) tumor cells based on the leave-one-out classification method where each Raman spectrum is tested against the rest of the data set.

Before Raman spectroscopy can be applied in the clinical setting, it is of central importance that its potential using preclinical animal models be investigated. We have designed a study to do this. We are currently investigating the use of Raman spectroscopy to assess response to radiation therapy in a preclinical animal (mouse) model, using 4T1 mouse breast cancer cells (see Sec. 2.A) and a TRAMP (Refs. 85 and 86) (Transgenic Adenocarcinoma of the Mouse Prostate) mouse model. Mice will be sacrificed at various time points following the irradiation exposure and tissues will be analyzed by

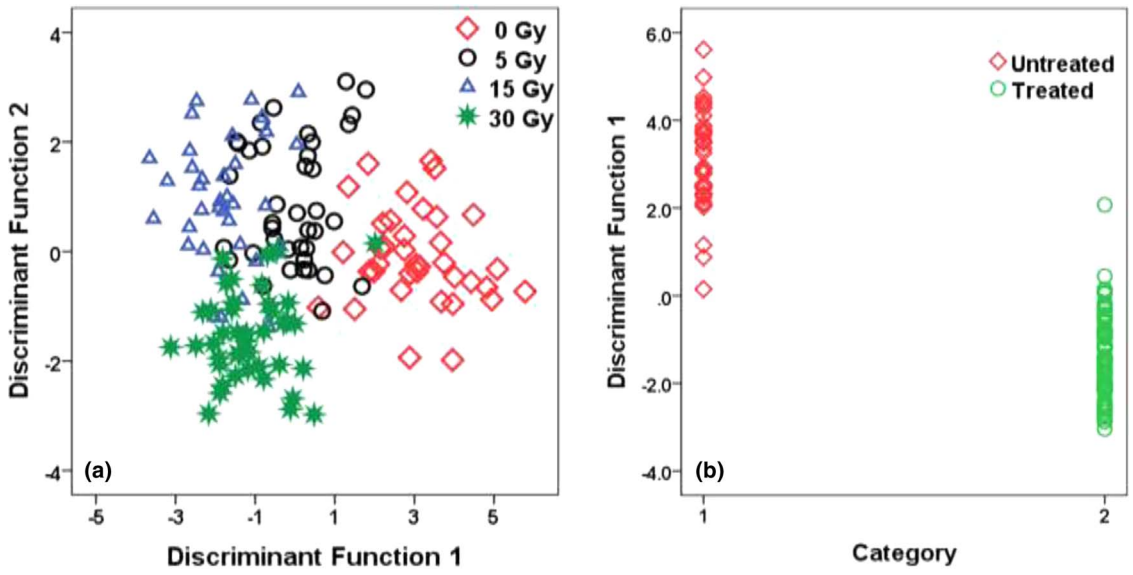

FIG. 8. (a) PCA/DFA analysis of the mouse breast cancer cell irradiation for 0, 5, 15, and 30 Gy. (b) DFA plot for considering only two groups, untreated (0 Gy) and treated (15 and 30 Gy).

pathologists. Raman measurements will be performed to determine tumor response and normal tissue damage to radiation at each time point.

3. LIMITATIONS, ADVANCES, AND THE FUTURE OF RAMAN SPECTROSCOPY

Raman spectroscopy detects the presence of specific molecules (proteins, lipids, carbohydrates, and nucleic acids) through their characteristic vibrational frequencies. It has the potential to measure up/down regulation of signaling proteins, epigenetic changes such as those associated with histone modifications, but less potential to measure methylation changes to the DNA. Consequently, Raman spectroscopy is not in competition to replace, but rather complimentary to modern mechanistically driven molecular biology cancer research. The inability to perform Raman measurements noninvasively (without tissue collection) for deep seated tumors is a major disadvantage for conventional Raman spectroscopic methods. However, emerging Raman techniques such as spatially offset Raman spectroscopy or transmission Raman spectroscopy could be utilized to achieve penetration depths up to centimeters.[87–89] Keller *et al.*[87] reported that the spatially offset Raman spectroscopy (SORP) offers proper depth sampling for intraoperative margin analysis for breast tumors. They developed a SORP probe with one source fiber at one end and ten collection fibers from 0.5 up to 3.5 mm distances in a ring formation with an increasing number of collection fibers. This design has increased the lateral sampling volume of the probe. The *in vitro* sample investigation of positive margins and negative margins following partial mastectomies was found to be 95% sensitive and 100% specific.[87] However, this is not an issue for skin cancers[47–49] and for *ex vivo* tissue investigations where Raman data can be collected readily from surgically removed tissue samples (biopsies) of interest as reported in many investigations. A bench top Raman spectrometer could also be integrated into the clinical setting to test fresh tissue biopsies *in vivo*.

Cancers associated with hollow organs such as colon, esophagus, stomach, and others have been investigated through a Raman probe without taking biopsies.[90–102] A fiber-optic Raman probe was used to conveniently reach a surface target and perform Raman measurements noninvasively using a miniaturized fiber-optic probe, which passes through the channels of medical endoscope. Wilson *et al.*[90,91] developed a Raman probe to determine gastrointestinal[92] and colonic polyps[93] during GI endoscopy. They were the first to report a human gastrointestinal tissue study, performed during routine clinical endoscopy in 2000. The spectral differences between normal and disease tissues appeared to be subtle due to a small dataset.[92] The later *ex vivo* and *in vivo* study of colon cancer showed overall accuracies greater than 93% for hyperplastic polyps and adenomatous polyps.[93] Recently, Wilson *et al.*[5,94] developed an experimental design to improve SERS imaging with the use of active nanoparticles. This wide-field quantitative multiplex SERS imaging design has the capability to perform biomarker-targeted real time Raman measurements. They are currently adapting this technology for an endoscope design to determine *in situ* SERS imaging.[5,94] Huang *et al.*[95] developed a Raman probe which has the capability of performing real time early cancer diagnosis in the gastrointestinal system during clinical endoscopic examination. They integrated a Raman endoscope into the clinical setting as an automated online Raman spectral diagnostic method. They performed Raman measurements on a series of tissues from many patients *in vivo*; mucosa, benign, and malignant ulcerous lesions in the stomach,[96] esophagus,[97] gastric cancer,[98] etc. and showed the potential of using a Raman probe in routine examinations. Stone *et al.*[99,100] developed a confocal Raman probe to use as an optical biopsy tool and tested their probe with normal, Barrett's esophagus, dysplasia, and cancer tissues at frozen state. The sensitivity and

specificity of the Raman spectral data in each pathology varied between 71%–81% and 81%–98%, respectively.

Zavaleta *et al.*[101] designed a Raman endoscope for SERS imaging with nanoparticles. They have performed a pilot study of usability of the Raman endoscope in humans during routine colonoscopy without nanoparticles as the regulatory approval for using nanoparticles is pending. Upon approval, they plan to administer nanoparticles topically and wash off the unbound nanoparticles. Ten different SERS nanoparticle flavors will be used to enhance different Raman modes. The Raman probe (5 mm in diameter) will be inserted through the accessory channel of a clinical endoscope to illuminate the targeted tumor area with a 785 nm laser beam and spectra will be acquired through the surrounding 36 fibers. This is a noncontact probe with a 10 mm working distance, which is a unique feature relative to other clinically used probes.[102] This will help mitigate issues associated with nonuniform surface topology of human tissue, imperfect centering during endoscopy, and user variability. They are hoping to test the Raman probe with nanoparticles in future studies.[101] These advances and future improvements in instrument technology will enable possible use of Raman spectroscopy for minimally invasive, real time diagnosis of cancer. Although, this technique is in its infancy, improvements in technology, and the increasing interest in research beginning with preclinical animal models might eventually lead to patient studies to test the feasibility of Raman spectroscopy for assessment of therapeutic response for both tumors and normal cells in solid tumors.

The state of the tissue, formalin fixed, formalin-fixed-paraffin processed, frozen, or fresh can influence the Raman spectral outcome. Fixing the tissues in formalin or embedding them in paraffin affects the biochemical composition of the tissue.[103,104] Biochemicals such as carotenoid or lipid are heavily affected in formalin fixed paraffin processed pediatric tissues.[72] Fixation of human bronchial tissues using formalin resulted in overall intensity reduction in Raman peaks.[103] Contamination of Raman spectral features due to paraffin wax residues was found at 1063, 1130, 1296, 1436, and 1465 cm^{-1}.[104] These Raman peaks should be removed from statistical analyses/models to avoid any contamination from wax residues if they are present in the Raman spectra. Raman intensity reduction was also observed in frozen human placenta tissues relative to fresh tissues.[104] Thus, the influence in the Raman spectral fingerprint depends upon both the state and the type of the tissue. An important aspect of diagnosis accuracy relies on the use of multivariate statistical analytical methods that are either commercially available or custom-built diagnostic algorithms. Statistical analyses such as principal component analysis, discriminant function analysis, support vector machine, partial least square regression, neural networks, or custom diagnostic algorithms are common among them. It is important to perform statistical analyses to capture the spectral changes as changes are often small, and extract the relevant Raman molecular information and automate the process of *in vivo* data collection. The sensitivity and specificity of the classification will be influenced by the level of distinguishability in Raman spectral features. Thus, classification/identification could be low due to subtle spectral differences or poorly resolved Raman spectra.

Moreover, statistical models/algorithms that predict unknown pathologies will immensely assist in efficient identification of a particular tissue. In fact, reference Raman spectra of pure chemical substances are needed to predict the existence of biochemicals unique to a tissue sample and/or to determine relative biochemical concentrations present in a target tissue. As the Raman spectrum consists of signatures arising from multiple chemical constituents in the target, some of the chemical fingerprints may overlap with peaks associated with other biochemicals, or can exist in a shoulder of a broad Raman peak. Thus, extracting unique biochemical fingerprints from the Raman spectra needs careful attention and is imperative in predicting the role of biochemicals in a certain pathology group. For these purposes, maintaining a large Raman spectral library of various tissue pathologies and pure substances is essential. Incorporating custom programs to extract the biochemical fingerprints from the Raman spectra is also vital for any Raman spectroscopic investigations.

In summary, the utilization of Raman spectroscopy as a diagnostic tool involves three major areas, (1) reduction of subjectivity of pathological diagnosis in situations where the assessment is uncertain and difficult and/or ability to provide complimentary molecular information, (2) ability to diagnose tumor, tumor progression, and the margins *in vivo* in real-time, and (3) ability to determine tumor response and normal tissue response to radiation therapy.

Histopathology is currently considered the gold standard method for disease identification. Allbrook *et al.*[105] reported that the interobserver reproducibility of Gleason grading of prostate cancer among 41 general pathologists in Georgia was in barely moderate agreement (overall kappa coefficient = 0.435). In addition, there were consistent undergrading of Gleason scores; 47% for Gleason scores 5–6 and 7. Pathologic diagnosis of oral dysplasia is often difficult.[106] Abbey *et al.*[107] conducted a study about reliability in diagnosing oral epithelial dysplasia among 6 board certified oral pathologists with 120 oral biopsies (without providing any clinical information). There were two phases for this investigation, in the first phase the pathologists were given 120 microscopic slides for review (mild, moderate, severe, or no epithelial dysplasia) and in the second phase 60 relabeled slides (out of 120) were given after several months. They found that the pathologists agreed with their own diagnoses only 50.8% of the time (within one histologic grade 92.4%) and the exact agreement with the sign-out diagnosis averaged 50.5% (within one histologic grade 90.4%). Abbey *et al.*[107] concluded that "accurate reproducible agreement among experienced board-certified oral pathologists diagnosing oral epithelial dysplasia is difficult to achieve." In a subsequent study, the clinical information was provided to improve the accuracy of diagnosis oral epithelial dysplasia for the same 120 slides.[108] These microscopic slides were provided to the same six pathologists after a year lapse of the previous study. The results showed that the exact agreement was reduced up to 20% and the identification

of presence or absence of epithelial dysplasia was reduced up to 23.4%. The accuracy and the consistency among six board certified pathologists were not improved in diagnosing oral epithelial dysplasia in this study.[108]

Second, real-time early stage diagnosis of cancer, and the possibility of assessment of surgical margins during the surgical procedure is an appealing approach. *In vivo* Raman spectroscopic evaluations provide quick analysis of the biomarkers responsible for the onset of a disease and/or their progression. The authors envision that this technique will provide an opportunity to save time and minimize the frequency of biopsy acquisition for pathological evaluations. Moreover, the surgeon will have molecular information about the positive margins of a cancer while the patient resides in the surgical bed, a process that is currently nonexistent. As new advances such as Raman probes become available,[49,90,95] the screening of superficial lesions or lesions associated with hollow organs will be immensely helpful for diagnosis of early stage cancers or the progression of tumors.

Third, the most influential application of the Raman technique in the field of radiation oncology is likely to be in the area of therapeutic response assessment. Due to the complexity of how tumors and normal tissues respond to radiation, histopathology may not provide (or predict) biomarkers related to tumor recurrence or normal tissue sequelae and the associated biochemical processes. We hypothesize that from the spectral outcome of Raman spectroscopy, which provides information on the mechanical and biochemical structure of cells, we will be able to identify changes in biomarkers pre- and postradiation therapy, that are linked to outcome (tumor response and normal tissue damage). While there is much work left to be done to prove this hypothesis, we anticipate, based on early *in vitro* experiments and preclinical animal studies, that there is high likelihood that we will be able to identify these biomarkers for certain types of cancers, much as we have demonstrated for diagnosis of cancer for head-and-neck and other cancers.[34,71,72] We propose that careful, pre-clinical, animal studies will be necessary to determine the efficacy of the Raman approach for response assessment. Thus, the Raman spectroscopy in the assessment of treatment response depends on the future animal trials and findings related to correlation of biomarkers/predictors to the clinical outcome as the question posed by Dr. Harold Varmus of NCI in one of the provocative questions last year.[31]

The authors believe that the future of the Raman spectroscopy in the context of early stage cancer detection and treatment response assessment is exciting. With recent and promised future technological developments, cancer patients might one day benefit from the ability of this technology to diagnose cancers at early stages and also to predict response of tumor and normal cells during or after radiation therapy. Indeed Dr. Harold Varmus, Director of the National Cancer Institute views the role of technologies enabling a better understanding of physical and mechanical properties of cells as central toward diagnosing cancers and assessing response, as evidenced in his "provocative question:" How can the physical properties of tumors, such as a cell's electrical, optical, or mechanical properties, be used to provide earlier or more reliable cancer detection, diagnosis, prognosis, or monitoring of drug response or tumor recurrence?

ACKNOWLEDGMENT

This project was supported in part by a grant from Varian Medical systems, Palo Alto, CA.

[a]Author to whom correspondence should be addressed. Electronic mail: sdevpur1@hfhs.org

[1]C. V. Raman, "A new type of secondary radiation," Nature (London) **121**(3048), 501–502 (1928).
[2]J. R. Ferraro, K. Nakamoto, and C. W. Brown, *Introductory Raman Spectroscopy* (Academic Press, Burlington, MA, 2002).
[3]S. Barbara, *Infrared Spectroscopy: Fundamentals and Applications* (Wiley, Hoboken, NJ, 2004).
[4]J. J. Laserna, *Modern Techniques in Raman Spectroscopy* (Wiley, England, 2006).
[5]P. Z. McVeigh, R. J. Mallia, I. Veilleux, and B. C. Wilson, "Widefield quantitative multiplex surface enhanced Raman scattering imaging in vivo," J. Biomed. Opt. **18**(4), 046011 (2013).
[6]M. E. Keating and H. J. Byrne, "Raman spectroscopy in nanomedicine: Current status and future prospective," Nanomedicine **8**(8), 1335–1351 (2013).
[7]S. Rahav and S. Mukamel, "Stimulated coherent anti-Stokes Raman scattering (CARS) resonances originate from double-slit interference of two-photon stokes pathways," Proc. Natl. Acad. Sci. U.S.A. **107**(11), 4825–4829 (2010).
[8]G. M. Cooper, *The Cell: A Molecular Approach* 2nd ed. (Sinauer Associates, Sunderland, MA, 2000).
[9]T. Strachan and A. P. Read, *Human Molecular Genetics*, 2nd ed. (Wiley-Liss, New York, 1999).
[10]J. T. Motz, M. Hunter, L. H. Galindo, J. A. Gardecki, J. R. Kramer, R. R. Dasari, and M. S. Feld, "Optical fiber probe for biomedical Raman spectroscopy," Appl. Opt. **43**(3), 542–554 (2004).
[11]U. Utzinger and R. R. Richards-Kortum, "Fiber optic probe for biomedical optical spectroscopy," J. Biomed. Opt. **8**(1), 121–147 (2003).
[12]A. Mahadaven-Jensen and R. Richards-Kortum, "Raman spectroscopy for cancer detection: A review," in *Proceedings of 19th Annual International Conference of the IEEE on Engineering in Medicine and Biology Society (IEEE-EMBS)* (IEEE, Chicago, IL, 1997), Vol. 6, pp. 2722–2727.
[13]R. S. Das and Y. K. Agrawal, "Raman spectroscopy: Recent advancements, techniques and applications," Vibrational Spectrosc. **57**, 163–176 (2011).
[14]M. D. Keller, E. M. Kanter, and A. Mahadevan-Jansen, "Raman spectroscopy for cancer diagnosis," Spectroscopy **21**(11), 33–41 (2006).
[15]A. Mahadevan-Jansen, M. F. Mitchell, N. Ramanujam, A. Malpica, S. Thomsen, U. Utzinger, and R. Richards-Kortum, "Near-infrared Raman spectroscopy for the diagnosis of cervical precancers," Photochem. Photobiol. **68**(1), 123–132 (1998).
[16]A. Cao, A. K. Pandya, G. K. Serhatkulu, R. E. Weber, H. Dai, J. S. Thakur, V. M. Naik, R. Naik, G. W. Auner, and R. J. Rabah, "A robust method for automated background subtraction of tissue fluorescence," J. Raman Spectrosc. **38**, 1199–1205 (2007).
[17]Z. Huang, A. McWilliams, H. Lui, D. I. McLean, S. Lam, and H. Zeng, "Near-infrared Raman spectroscopy for optical diagnosis of lung cancer," Int. J. Cancer **107**(6), 1047–1052 (2003).
[18]E. B. Hanlon, R. Manoharan, T. W. Koo, K. E. Shafer, J. T. Motz, M. Fitzmaurice, J. R. Kramer, I. Itzkan, R. R. Dasari, and M. S. Feld, "Prospects for in vivo Raman spectroscopy," Phys. Med. Biol. **45**(2), R1–R59 (2000).
[19]Z. Movasaghi, S. Rehman, and I. U. Rehman, "Raman spectroscopy of biological tissues," Appl. Spectrosc. **42**, 493–541 (2007).
[20]J. De Gelder, K. De Gussem, P. Vandenabeele, and L. Moens, "Reference database f Raman spectra of biological molecules," J. Raman Spectrosc. **38**, 1133–1147 (2007).
[21]C. J. Frank and R. L. McCreery, "Raman spectroscopy of normal and diseased human breast tissues," Anal. Chem. **67**, 777–783 (1995).
[22]A. S. Haka, K. E. Shafer-Peltier, M. Fitzmaurice, J. Crowe, R. R. Dasari, and M. S. Feld, "Diagnosing breast cancer by using Raman spectroscopy," Proc. Natl. Acad. Sci. U.S.A. **102**, 12371–12376 (2005).

[23]I. T. Jolliffe, *Principal Components Analysis*, 2nd ed. (Springer-Verlag, New York, 2002).
[24]W. R. Klecka, *Discriminant Analysis, Series: Quantitative Applications in the Social Sciences* (Sage, Newbury Park, 1980).
[25]J. Mazanec, M. Melišek, M. Oravec, and J. Pavlovičová, "Support vector machines, PCA and LDA in face recognition," J. Electr. Eng. **59**(4), 203–209 (2008).
[26]C. M. Bishop, *Neural Networks for Pattern Recognition*, 3rd ed. (Oxford University Press, USA, 1995).
[27]L. A. Nafie, "Recent advances in linear and nonlinear Raman spectroscopy. Part VI," J. Raman Spectrosc. **43**, 1845–1863 (2012).
[28]C. Mallidis, V. Sanchez, J. Wistuba, F. Wuebbeling, M. Burger, C. Fallinich, and S. Schlatt, "Raman microspectroscopy: shining a new light on reproductive medicine," Human Reproduction Update **0**(0), 1–12 (2013).
[29]C. Kallaway, L. M. Almond, H. Barr, J. Wood, J. Hutchings, C. Kendall, and N. Stone, "Advances in clinical application of Raman spectroscopy for cancer diagnostics," Photodiagnosis Photodyn. Ther. **10**, 207–219 (2013).
[30]H. G. Schulze, C. J. Barbosa, L. S. Greek, R. F. B. Turner, C. A. Haynes, K.-F. Klein, and M. W. Blades, "Advances in fiber-optic based UV resonance Raman spectroscopy techniques for anatomical and physiological investigations," Proc. SPIE **3608**, 157–166 (1999).
[31]http://provocativequestions.nci.nih.gov/archived-rfas-and-pqs/rfa-archive-2012/mainquestions_listview?mqCategory=Group+C.
[32]P. Crow, N. Stone, C. A. Kendall, J. S. Uff, J. A. M. Barr, and M. Wright, "The use of Raman spectroscopy to identify and grade prostatic adenocarcinoma in vitro," Br. J. Cancer **89**(1), 106–108 (2003).
[33]P. Crow, A. Molckovsky, N. Stone, J. Uff, B. Wilson, and L. M. Wong-KeeSong, "Assessment of fiberoptic near-infrared Raman spectroscopy for diagnosis of bladder and prostate cancer," Urology **65**(6), 1126–1130 (2005).
[34]S. Devpura, J. S. Thakur, F. H. Sarkar, W. A. Sakr, V. M. Naik, and R. Naik, "Detection of benign epithelia, prostatic Intraepithelial neoplasia, and cancer regions in radical prostatectomy tissues using Raman spectroscopy," Vibrational Spectrosc. **53**, 227–232 (2010).
[35]N. Stone, C. Kendall, J. Smith, P. Crow, and H. Barr, "Raman spectroscopy for identification of epithelial cancers," Faraday Discuss. **126**, 141–157 (2004).
[36]A. S. Haka, Z. Volynskaya, J. Gardecki, J. Nazemi, J. Lyons, D., Hicks, M. Fitzmaurice, R. R. Dasari, J. P. Crowe, and M. S. Feld, "In vivo margin assessment during partial mastectomy breast surgery using Raman spectroscopy," Cancer Res. **66**, 3317–3322 (2006).
[37]A. S. Haka, Z. Volynskaya, J. Gardecki, J. Nazemi, R. Shenk, N. Wang, R. R. Dasari, M. Fitzmaurice, and M. S. Feld, "Diagnosing breast cancer using Raman spectroscopy: Prospective analysis," J. Biomed. Opt. **14**, 054023 (2009).
[38]A. Mahadevan-Jansen and R. R. Richards-Kortum, "Raman spectroscopy for the detection of cancers and precancers," J. Biomed. Opt. **1**(1), 31–70 (1996).
[39]S. K. Majumder, F. I. Boulos, M. C. Kelley, A. Mahadevan-Jansen, and M. D. Keller, "Comparison of autofluorescence, diffuse reflectance, and Raman spectroscopy for breast tissue discrimination," J. Biomed. Opt. **13**(5), 054009 (2008).
[40]N. Stone, C. Kendall, N. Shepherd, P. Crow, and H. Barr, "Near-infrared Raman spectroscopy for the classification of epithelial pre-cancers and cancers," J. Raman Spectrosc. **33**, 564–573 (2002).
[41]P. Crow, J. S. Uff, J. A. Farmer, M. P. Wright, and N. Stone, "The use of Raman spectroscopy to identify and characterize transitional cell carcinoma in vitro," BJU Int. **93**(9), 1232–1236 (2004).
[42]S. Koljenovic, L.-P. Choo-Smith, T. C. B. Schut, J. M. Kros, H. J. van den Berge, and J. G. Puppels, "Discriminating vital tumor from necrotic tissue in human glioblastoma tissue samples by Raman spectroscopy," Lab. Invest. **82**, 1265–1277 (2002).
[43]C. Krafft, S. B. Sobottka, G. Schackert, and R. Salzer, "Near infrared Raman spectroscopic mapping of native brain tissue and intracranial tumors," Analyst **130**, 1070–1077 (2005).
[44]S. Koljenović, T. C. B. Schut, A. Vincent, J. M. Kros, and G. J. Puppels, "Detection of meningioma in dura mater by Raman spectroscopy," Anal. Chem. **77**(24), 7958–7965 (2005).
[45]K. Gajjar, L. D. Heppenstall, W. Pang, K. M. Ashton, J. Trevisan, I. I. Patel, V. Llabjani, H. F. Stringfellow, P. L. Martin-Hirsch, T. Dawsonb, and F. L. Martin, "Diagnostic segregation of human brain tumours using Fourier-transform infrared and/or Raman spectroscopy coupled with discriminant analysis," Anal. Methods **5**, 89–102, (2013).
[46]S. N. Kalkanis, R. E. Kast, M. L. Rosenblum, T. Mikkelsen, S. M. Yurgelevic, K. M. Nelson, A. Raghunathan, L. M. Poisson, and G. W. Auner, "Raman spectroscopy to distinguish grey matter, necrosis, and glioblastoma multiforme in frozen tissue sections," Neurooncol. **116**(3), 477–485 (2014).
[47]A. Nijssen, T. C. B. Schut, F. Heule, P. J. Caspers, D. P. Hayes, M. H. Neumann, and G. J. Puppels, "Discriminating basal cell carcinoma from its surrounding tissue by Raman spectroscopy," J. Invest. Dermatol. **119**(1), 64–69 (2002).
[48]H. Lui, J. Zhao, D. McLean, and H. Zeng, "Real-time Raman spectroscopy for in vivo skin cancer diagnosis," Cancer Res. **72**(10), 2491–500 (2012).
[49]Article appeared in Forbes, see http://www.forbes.com/sites/johnnosta/2013/03/14/simply-amazing-instantly-diagnosis-melanoma-with-the-flash-of-a-light/.
[50]C. A. Lieber, S. K. Majumder, D. L. Ellis, D. D. Billheimer, and A. Mahadevan-Jansen, "In vivo nonmelanoma skin cancer diagnosis using Raman microspectroscopy," Lasers Surg. Med. **40**, 461–467 (2008).
[51]Article appeared in medphysweb.org, see http://medicalphysicsweb.org/cws/article/newsfeed/56110.
[52]X. Qian, X.-H. Peng, D. O. Ansari, Q. Yin-Goen, G. Z. Chen, D. M. Shin, L. Yang, A. N. Young, M. D. Wang, and S. Nie, "In vivo tumor targeting and spectroscopic detection with surface-enhanced Raman nanoparticle tags," Nat. Biotechnol. **26**(1), 83–90 (2008).
[53]T. Vo-Dinh, L. R. Allain, and D. L. Stokes, "Cancer gene detection using surface-enhanced Raman scattering (SERS)," J. Raman Spectrosc. **33**, 511–516 (2002).
[54]H. Kim, K. M. Kosuda, R. P. Van Duynea, and P. C. Stair, "Resonance Raman and surface-and tip-enhanced Raman spectroscopy methods to study solid catalysts and heterogeneous catalytic reactions," Chem. Soc. Rev. **39**, 4820–4844 (2010).
[55]P. J. Caspers, G. W. Lucassen, and G. J. Puppels, "Combined *in vivo* confocal Raman spectroscopy and confocal microscopy of human skin," Biophys. J. **85**, 572–580 (2003).
[56]J. Choi, J. Choo, H. Chung, D.-G. Gweon, J. Park, H. J. Kim, S. Park, and C.-H. Oh, "Direct observation of spectral differences between normal and basal cell carcinoma (BCC) tissues using confocal Raman microscopy," Biopolymers **77**, 264–272 (2005).
[57]H. Wang, Y. Fu, P. Zickmund, R. Shi, and J.-X. Cheng, "Coherent anti-Stokes Raman scattering imaging of axonal myelin in live spinal tissues," Biophys. J. **89**(1), 581–591 (2005).
[58]C. L. Evans and X. S. Xie, "Coherent anti-Stokes Raman scattering microscopy: Chemical imaging for biology and medicine," Rev. Anal. Chem. **1**, 883–909 (2008).
[59]R. Manoharan, Y. Wang, R. R. Dasari, S. S. Singer, R. P. Rava, and M. S. Feld, "Ultraviolet resonance Raman spectroscopy for detection of colon cancer," Laser Life Sci. **6**(4), 217–227 (1995).
[60]N. N. Boustany, R. Manoharan, R. R. Dasari, and M. S. Feld, "Ultraviolet resonance Raman spectroscopy of bulk and microscopic human colon tissue," Appl. Spectrosc. **54**(1), 24–30 (2000).
[61]M. Ji, D. A. Orringer, C. W. Freudiger, S. Ramkissoon, X. Liu, D. Lau, A. J. Golby, I. Norton, M. Hayashi, N. Y. R. Agar, G. S. Young, C. Spino, S. Santagata, S. Camelo-Piragua, K. L. Ligon, O. Sagher, and X. S. Xie, "Rapid, label-free detection of brain tumors with stimulated Raman scattering microscopy," Sci. Transl. Med. **5**, 201ra119 (2013).
[62]C. M. Krishna, G. D. Sockalingum, J. Kurien, L. Rao, L. Venteo, M. Pluot, and V. B. Kartha, "Micro-Raman spectroscopy for optical pathology of oral squamous cell carcinoma," Appl. Spectrosc. **58**(9), 1128–1135 (2004).
[63]R. Malini, K. Venkatakrishna, J. Kurien, K. M. Pai, L. Rao, V. B. Kartha, and C. M. Krishna, "Discrimination of normal, inflammatory, premalignant, and malignant oral tissue: A Raman spectroscopy study," Biopolymers **81**, 179–193 (2006).
[64]E. Vargis, E. M. Kanter, S. K. Majumder, M. D. Keller, R. B. Beaven, G. G. Raod, and A. Mahadevan-Jansen, "Effect of normal variations on disease classification of Raman spectra from cervical tissue," Analyst **136**, 2981–2987 (2011).
[65]C. M. Krishna, N. B. Prathima, R. Malini, B. M. Vadhiraja, R. A. Bhatt, D. J. Fernandes, P. Kushtagi, M. S. Vidyasagar, and V. B. Kartha, "Raman spectroscopy studies for diagnosis of cancers in human uterine cervix," Vib. Spectrosc. **41**, 136–141 (2006).
[66]U. Utzinger, A. Mahadevan-Jansen, D. Hinzelman, M. Follen, and R. Richards-Kortum, "Near Infrared Raman Spectroscopy for In Vivo

Detection of Cervical Precancers," Applied Spectroscopy **55**(8), 955–959 (2001).
[67]Y.-K. Min, T. Yamamoto, E. Kohda, T. Ito, and H.-o. Hamaguchi, "1064 nm near-infrared multichannel Raman spectroscopy of fresh human lung tissues," J. Raman Spectrosc. **36**, 73–76 (2005).
[68]G. Shetty, C. Kendall, N. Shepherd, N. Stone, and H. Barr, "Raman spectroscopy: Elucidation of biochemical changes in carcinogenesis of oesophagus,"Br. J. Cancer **94**, 1460–1464 (2006).
[69]D. P. Lau, Z. Huang, H. Lui, C. S. Man, K. Berean, M. D. Morrison, and H. Zeng, "Raman spectroscopy for optical diagnosis in normal and cancerous tissue of the nasopharynx—Preliminary findings," Lasers Surg. Med. **32**, 210–214 (2003).
[70]D. P. Lau, Z. Huang, H. Lui, D. W. Anderson, D. W., K. Berean, M. D. Morrison, L. Shen, and H. Zeng, "Raman spectroscopy for optical diagnosis in the larynx: Preliminary findings," Lasers Surg. Med. **37**, 192–200 (2005).
[71]S. Devpura, J. S. Thakur, S. Sethi, V. M. Naik, and R. Naik, "Diagnosis of head and neck squamous cell carcinoma using Raman spectroscopy: Tongue tissues," J. Raman Spectrosc. **43**, 490–496 (2012).
[72]S. Devpura, J. S. Thakur, J. M. Poulik, R. Rabah, V. M. Naik, and R. Naik, "Raman spectroscopic investigation of frozen and formalin-fixed paraffin processed tissues of pediatric tumors: Neuroblastoma and ganglioneuroma," J. Raman Spectrosc. **44**(3), 370–376 (2013).
[73]B. Emami, J. Lyman, A. Brown, L. Coia, M. Goitein, J. E. Munzenrider, B. Shank, L. J. Solin, and M. Wesson, "Tolerance of normal tissue to therapeutic irradiation," Int. J. Radiat. Oncol., Biol., Phys. **21**(1), 109–22 (1991).
[74]S. M. Bentzen, L. S. Constine, J. O. Deasy, A. Eisbruch, A. Jackson, L. B. Marks, R. K. T. Haken, and E. D. Yorke, "Quantitative analyses of normal tissue effects in the clinic (QUANTEC): An introduction to the scientific issues," Int. J. Radiat. Oncol., Biol., Phys. **76**(3), S3–S9 (2010).
[75]P. Okunieff, Y. Chen, D. J. Maguire, and A. K. Huser, "Molecular markers of radiation-related normal tissue toxicity," Cancer Metastasis Rev. **27**(3), 363–374 (2008).
[76]Q. Matthews, A. Jirasek, J. Lum, X. Duan, and A. G. Brolo, "Variability in Raman spectra of single human tumor cells cultured in vitro: Correlation with cell cycle and culture confluency," Appl. Spectrosc. **64**, 871–887 (2010).
[77]Q. Matthews, A. Jirasek, J. Lum, X. Duan, and A. G. Brolo, "Biochemical signatures of in vitro radiation response in human lung, breast and prostate tumour cells observed with Raman spectroscopy," Phys. Med. Biol. **56**, 6839–6855 (2011).
[78]R. J. Lakshmi, M. Alexander, J. Kurien, K. K. Mahato, and V. B. Kartha, "Osteoradionecrosis (ORN) of the mandible: A laser Raman spectroscopic study," Appl. Spectrosc. **57**(9), 1100–1116 (2003).
[79]M. S. Vidyasagar, K. Maheedhar, B. M. Vadhiraja, D. J. Fernendes, V. B. Kartha, and C. M. Krishna, "Prediction of radiotherapy response in cervix cancer by Raman spectroscopy: A pilot study," Biopolymers **89**, 530–537 (2008).
[80]R. J. Lakshmi, V. B. Karth, C. M. Krishna, J. G. R. Solomon, G. Ullas, and P. U. Devi, "Tissue Raman spectroscopy for the study of radiation damage: Brain irradiation of mice," Radiat. Res. **157**(2), 175–182 (2002).
[81]B. Gong, M. E. Oest, K. A. Mann, T. A. Damron, and M. D. Morris, "Raman spectroscopy demonstrates prolonged alteration of bone chemical composition following extremity localized irradiation," Bone **57**(1), 252–258 (2013).
[82]H. D. Barth, E. A. Zimmermann, E. Schaible, S. Y. Tang, T. Alliston, and R. O. Ritchie, "Characterization of the effects of x-ray irradiation on the hierarchical structure and mechanical properties of human cortical bone," Biomaterials **32**(34), 8892–8904 (2011).
[83]C. N. Tchanque-Fossuo, B. Gong, B. Poushanchi, A. Donneys, D. Sarhaddi, K. K. Gallagher, S. S. Deshpande, S. A. Goldstein, M. D. Morris, and S. R. Buchman, "Raman spectroscopy demonstrates Amifostine induced preservation of bone mineralization patterns in the irradiated murine mandible," Bone **52**(2), 712–717 (2013).
[84]I. Notingher, "Raman spectroscopy cell-based biosensors," Sensor **7**, 1343–1358 (2007).
[85]N. M. Greenberg, F. DeMayo, M. J. Finegold, D. Medina, W. D. Tilley, J. O. Aspinall, G. R. Cunha, A. A. Donjacour, R. J. Matusik, and J. M. Rosen, "Prostate cancer in a transgenic mouse," Proc. Natl. Acad. Sci. U.S.A. **92**(8), 3439–3443 (1995).
[86]J. R. Gingrich, R. J. Barrios, B. A. Morton, B. F. Boyce, F. J. DeMayo, M. J. Finegold, R. Angelopoulou, J. M. Rosen, and N. M. Greenberg, "Metastatic prostate cancer in a transgenic mouse," Cancer Res. **56**(18), 4096–102 (1996).
[87]M. D. Keller, E. Vargis, N. de Matos Granja, R. H. Wilson, M. A. Mycek, M. C. Kelley, and A. Mahadevan-Jansen, "Development of a spatially offset Raman spectroscopy probe for breast tumor surgical margin evaluation," J. Biomed. Opt. **16**(7), 077006 (2011).
[88]M. V. Schulmerich, J. H. Cole, K. A. Dooley, M. D. Morris, J. M. Kreider, S. A. Goldstein, S. Srinivasan, and B. W. Pogue, "Noninvasive Raman tomographic imaging of canine bone tissue," J. Biomed. Opt. **13**(2), 020506 (2008).
[89]P. Matousek and N. Stone, "Recent advances in the development of Raman spectroscopy for deep non-invasive medical diagnosis," J. Biophotonics **6**(1), 7–19 (2013).
[90]M. G. Shim and B. C. Wilson, "Development of an In Vivo Raman Spectroscopic System for Diagnostic Applications," J. Raman Spectrosc. **28**, 131–142 (1997).
[91]M. G. Shim, B. C. Wilson, E. Marple, and M. Wach, "Study of fiber optic probes for in vivo medical Raman spectroscopy," Appl. Spectrosc. **53**, 619–627 (1999).
[92]M. G. Shim, L.-M. W. K. Song, N. E. Marcon, and B. C. Wilson, "In vivo near-infrared Raman spectroscopy: Demonstration of feasibility during clinical gastrointestinal endoscopy," Photochem. Photobiol. **72**, 146–150 (2000).
[93]A. Molckovsky, L. M. Song, M. G. Shim, N. E. Marcon, and B. C. Wilson, "Diagnostic potential of near-infrared Raman spectroscopy in the colon: Differentiating adenomatous from hyperplastic polyps," Gastrointest. Endosc. **57**(3), 396–402 (2003).
[94]R. J. Mallia, P. Z. McVeigh, I. Veilleux, and B. C. Wilson, "Filter-based method for background removal in high-sensitivity wide-field-surface-enhanced Raman scattering imaging in vivo," J. Biomed. Opt. **17**(7), 076017 (2012).
[95]M. S. Bergholt, W. Zheng, K. Y. Ho, K. G. Yeoh, and Z. Huang, "Raman Endoscopy for Objective Diagnosis of Early Cancer in the Gastrointestinal System," J Gastroint. Dig. Syst. S1:008 (2013).
[96]M. S. Bergholt, W. Zheng, K. Lin, K. Y. Ho, M. Teh, K. G. Yeoh, J. B. So, and Z. Huang, "Raman endoscopy for in vivo differentiation between benign and malignant ulcers in the stomach," Analyst **135**, 3162–3168 (2010).
[97]M. S. Bergholt, W. Zheng, K. Lin, K. Y. Ho, M. Teh, J. B. So, A. Shabbir, and Z. Huang, "In vivo diagnosis of esophageal cancer using image-guided Raman endoscopy and biomolecular modeling," Technol. Cancer Res. Treat. **10**, 103–112 (2011).
[98]S. Duraipandian, M. S. Bergholt, W. Zheng, K. Y. Ho, M. Teh, K. G. Yeoh, J. B. Y. So, A. Shabbir, and Z. Huang, "Real-time Raman spectroscopy for in vivo, online gastric cancer diagnosis during clinical endoscopic examination," J. Biomed. Opt. **17**(8), 081418 (2012).
[99]J. C. Day, R. Bennett, B. Smith, C. Kendall, J. Hutchings, G. M. Meaden, C. Born, S. Yu, and N. Stone, "A miniature confocal Raman probe for endoscopic use," Phys. Med. Biol. **54**, 7077–7087 (2009).
[100]C. Kendall, J. Day, J. Hutchings, B. Smith, N. Shepherd, H. Barr, and N. Stone, "Evaluation of Raman probe for oesophageal cancer diagnostics," Analyst **135**, 3038–3041 (2010).
[101]C. L. Zavaleta, E. Garai, J. T. C. Liu, S. Sensarn, M. J. Mandella, D. Van de Sompel, S. Friedland, J. Van Dam, C. H. Contag, and S. S. Gambhir, "A Raman-based endoscopic strategy for multiplexed molecular imaging," Proc. Natl. Acad. Sci. U.S.A. **110**(25), E2288–E2297 (2013).
[102]E. Garai, S. Sensarn, C. L. Zavaleta, D. Van de Sompel, N. O. Loewke, M. J. Mandella, S. S. Gambhir, and C. H. Contag, "High-sensitivity, real-time, ratiometric imaging of surface-enhanced Raman scattering nanoparticles with a clinically translatable Raman endoscope device," J. Biomed. Opt. **18**(9), 096008 (2013).
[103]Z. Huang, A. McWilliams, S. Lam, J. English, D. I. McLean, H. Lui, and H. Zeng, "Effect of formalin fixation on the near-infrared Raman spectroscopy of normal and cancerous human bronchial tissues," Int. J. Oncol. **23**(3), 649–655 (2003).
[104]E. O'Faolaoin, M. Hunter, J. Byrne, P. Kellehan, M. McNamara, H. Byrne, and F. Lyng, "A study examining the effects of tissue processing on human tissue sections using vibrational spectroscopy," Vibrational Spec. **38**(1–2), 121–127 (2005).
[105]W. C. Allsbrook, K. A. Mangold, M. H. Johnson, R. B. Lane, C. G. Lane, and J. I. Epstein, "Interobserver reproducibility of Gleason grading of prostatic carcinoma: General pathologists," Human Pathol. **32**(1), 81–88 (2001).

[106]F. Dost, K. A. Lê Cao, P. J. Ford, and C. S. Farah, "A retrospective analysis of clinical features of oral malignant and potentially malignant disorders with and without oral epithelial dysplasia," Oral Surg. Oral Med. Oral Pathol. Oral Radiol. **116**, 725–733 (2013).
[107]L. M. Abbey, G. E. Kaugars, J. C. Gunsolley, J. C. Burns, D. G. Page, J. A. Svirsky, E. Eisenberg, D. J. Krutchkoff, and M. Cushing, "Intraexaminer and interexaminer reliability in the diagnosis of oral epithelial dysplasia," Oral Surg. Oral Med. Oral Pathol. Oral Radiol. Endod. **80**(2), 188–191 (1995).
[108]L. M. Abbey, G. E. Kaugars, J. C. Gunsolley, J. C. Burns, D. G. Page, J. A. Svirsky, E. Eisenberg, and D. J. Krutchkoff, "The effect of clinical information on the histopathologic diagnosis of oral epithelial dysplasia," Oral Surg. Oral Med. Oral Pathol. Oral Radiol. Endod. **85**(1), 74–77 (1998).